Gene Expression **2026** vol. 25(3) | e00023
DOI: 10.14218/GE.2026.00023

Original Article

Clinical–Inflammatory Phenotypes and Circulating *hsa_circ_101555* Along the Cirrhosis–Hepatocellular Carcinoma Continuum: A Cross-sectional Study

Nourhan Badwei[1*], Amal Tohamy Abdel Moez[1], Houssam El-Deen M. Salem[1], Nashwa El-Khazragy[2] and Mohammed Soliman Gado[1]

[1]*Department of Tropical Medicine, Gastroenterology and Hepatology, Faculty of Medicine, Ain Shams University, Cairo, Egypt;* [2]*Department of Clinical Pathology, Faculty of Medicine, Ain Shams University, Cairo, Egypt*

Received: June 26, 2026 | **Revised:** July 12, 2026 | **Accepted:** July 28, 2026 | **Published online:** July 29, 2026

Abstract

Background and objectives: The clinical spectrum from cirrhosis to hepatocellular carcinoma (HCC) reflects interactions among hepatic dysfunction, systemic inflammation, and tumor burden. Whether circulating biomarkers add value beyond clinical parameters remains uncertain. This study aimed to evaluate an exploratory Model for End-Stage Liver Disease (MELD)–neutrophil-to-lymphocyte ratio (NLR)-based clinical–inflammatory phenotyping framework for discriminating advanced HCC features and to determine whether circulating *hsa_circ_101555* provides incremental discriminatory value beyond this framework.

Methods: This single-center cross-sectional study included 92 consecutive patients (30 with cirrhosis without HCC and 62 with HCC). Patients were classified into three exploratory clinical–inflammatory phenotypes using a hierarchical MELD–NLR algorithm (Phenotype I, n = 25; II, n = 33; III, n = 34). Circulating *hsa_circ_101555* was quantified by reverse transcription quantitative polymerase chain reaction. Receiver operating characteristic analysis evaluated Barcelona Clinic Liver Cancer stage C among patients with HCC (n = 62; events = 28). Internal validation used bootstrap resampling.

Results: Higher-risk phenotypes included progressively larger proportions of patients with HCC and greater frequencies of advanced tumor characteristics. The combined MELD–NLR model showed the highest discrimination (the area under the receiver operating characteristic curve (AUC) 0.90; 95% confidence interval 0.82–0.97), with 85.7% sensitivity, 82.4% specificity, and 83.9% accuracy. This performance exceeded that of NLR alone (AUC, 0.80) and MELD alone (AUC, 0.77). Circulating *hsa_circ_101555* was associated with smaller tumors and an earlier Barcelona Clinic Liver Cancer stage but showed modest discrimination (AUC, 0.69) and did not improve the MELD–NLR model (ΔAUC = 0.002; DeLong P = 0.79).

Conclusions: The exploratory MELD–NLR-based clinical–inflammatory framework identifies patient groups with differing frequencies of advanced HCC features. Circulating *hsa_circ_101555* provides no incremental discriminatory value beyond routinely available clinical–inflammatory parameters and requires external validation before clinical use.

Keywords: Liver cirrhosis; Hepatocellular carcinoma; Clinical–inflammatory phenotype; MELD; Neutrophil-to-lymphocyte ratio; *hsa_circ_101555*; Circular RNA.

***Correspondence to:** Nourhan Badwei, Department of Tropical Medicine, Gastroenterology and Hepatology, Hepatoma group, Faculty of Medicine, Ain Shams University, Cairo 11517, Egypt. ORCID: https://orcid.org/0000-0002-7658-2591. Tel: +20-11-1533-4136, E-mail: nourhanbadwei1990@gmail.com

How to cite this article: Badwei N, Moez ATA, Salem HEDM, El-Khazragy N, Gado MS. Clinical–Inflammatory Phenotypes and Circulating *hsa_circ_101555* Along the Cirrhosis–Hepatocellular Carcinoma Continuum: A Cross-sectional Study. *Gene Expr* 2026;25(3):e00023. DOI: https://doi.org/10.14218/GE.2026.00023.

Introduction

Disease progression along the cirrhosis–hepatocellular carcinoma (HCC) continuum is highly heterogeneous, reflecting complex interactions among hepatic dysfunction, systemic inflammation, and tumor biology. Cirrhosis represents the final common pathway of chronic liver disease and constitutes the principal substrate for HCC, one of the leading causes of cancer-related

© 2026 The Author(s). This article has been published under the terms of Creative Commons Attribution-Noncommercial 4.0 International License (CC BY-NC 4.0), which permits noncommercial unrestricted use, distribution, and reproduction in any medium, provided that the following statement is provided. "This article has been published in *Gene Expression* at https://doi.org/10.14218/GE.2026.00023 and can also be viewed on the Journal's website at https://www.xiahepublishing.com/journal/ge".

mortality worldwide.[1-3] Consequently, patients with apparently similar clinical stages may exhibit markedly different disease characteristics, highlighting the need for integrated approaches to clinical assessment.

Conventional clinical scoring systems, including the Child–Pugh classification and the Model for End-Stage Liver Disease (MELD), provide robust assessments of hepatic reserve but do not fully capture systemic inflammatory status or tumor-related biological heterogeneity.[4,5] Likewise, tumor staging systems such as the Barcelona Clinic Liver Cancer (BCLC) classification describe tumor burden, liver function, performance status, and treatment allocation but do not directly incorporate systemic inflammatory biomarkers.[6,7] Increasing evidence suggests that systemic inflammation is closely associated with both cirrhosis severity and hepatocarcinogenesis,[8,9] and inflammatory indices such as the neutrophil-to-lymphocyte ratio (NLR) have consistently been associated with adverse tumor characteristics in HCC.[10]

In parallel, circulating molecular biomarkers have emerged as potential adjuncts for improving disease characterization. Among these, circular RNAs (circRNAs) have attracted considerable interest because of their relative molecular stability and potential regulatory roles in HCC biology. Experimental studies suggest that *hsa_circ_101555* may participate in pathways related to cellular proliferation, migration, and tumor progression. Nevertheless, despite promising biological evidence, its incremental clinical value beyond routinely available laboratory parameters remains uncertain.[11-13]

It remains unclear whether molecular biomarkers provide clinically meaningful incremental information beyond integrated clinical assessment or whether they primarily reflect underlying biological variation without improving discrimination of clinically relevant disease features. Addressing this question may help translate molecular findings into clinical applications.

In previous phases of our translational research program, circulating *hsa_circ_101555* showed diagnostic and biological associations in separate cohorts of patients with chronic liver disease and HCC.[12,13] The present study was an integrated secondary analysis of these previously reported cohorts and aimed to evaluate an exploratory clinical–inflammatory framework integrating hepatic dysfunction and systemic inflammatory activity along the cirrhosis–HCC continuum and determine whether circulating *hsa_circ_101555* provides incremental cross-sectional discriminatory value beyond this framework for identifying advanced HCC features.

Materials and methods

Study design and population

This investigator-initiated, single-center, cross-sectional study was an exploratory secondary analysis of prospectively collected data from a translational research program investigating clinical–inflammatory phenotyping and the incremental value of circulating *hsa_circ_101555* along the cirrhosis–HCC continuum.[12,13]

Previous phases of this research program evaluated the associations of serum-derived *hsa_circ_101555* expression with HCC detection and chronic liver disease characteristics in separate patient populations.[12,13] The present phase differs from previous investigations by integrating an exploratory clinical–inflammatory phenotyping framework based on routinely available clinical parameters with molecular biomarker assessment to determine whether *hsa_circ_101555* provides incremental discriminatory information beyond established clinical and inflammatory variables.

The study was conducted at Ain Shams University Hospitals, Cairo, Egypt, during May 2023–April 2024. Consecutive adult patients attending the Tropical Medicine Department during the study period were screened for eligibility. A total of 92 patients fulfilled the eligibility criteria and were included in the final analysis, comprising 30 patients with cirrhosis without HCC and 62 patients with radiologically confirmed HCC.

Cirrhosis was diagnosed based on clinical, laboratory, radiological, and/or endoscopic evidence of chronic liver disease and portal hypertension.

Hepatocellular carcinoma was diagnosed according to European Association for the Study of the Liver and American Association for the Study of Liver Diseases imaging criteria, based on multiphasic contrast-enhanced computed tomography and/or magnetic resonance imaging showing arterial-phase hyperenhancement with portal venous or delayed washout. BCLC staging was assigned before initiation of HCC-specific treatment according to the contemporary BCLC classification.[6,14,15]

Eligible participants were adults aged ≥18 years with complete clinical, laboratory, radiological, and molecular data. Patients were excluded if they had active bacterial infection at enrollment, autoimmune or systemic inflammatory disorders, hematological diseases affecting leukocyte or platelet counts, extrahepatic malignancy, previous systemic anticancer therapy, liver transplantation, pregnancy, or incomplete clinical or laboratory data.

Participant recruitment, eligibility assessment, and final cohort allocation are illustrated in Supplementary Fig. 1.

Accordingly, this analysis addressed a distinct objective: whether circulating *hsa_circ_101555* provides incremental discriminatory information beyond an integrated clinical–inflammatory framework along the cirrhosis–HCC continuum.

Clinical, laboratory, and radiological assessment

All participants underwent standardized clinical, laboratory, and radiological evaluation at baseline before initiation of HCC-specific treatment. Demographic characteristics, medical history, and clinical findings were recorded.

Laboratory investigations included complete blood count, liver function tests, renal function tests, coagulation profile, serum alpha-fetoprotein (AFP), and C-reactive protein (CRP). Hepatic functional reserve was assessed using the Child–Pugh classification, MELD score, and Albumin–Bilirubin (ALBI) grade.[4,5,16,17]

Systemic inflammatory status was evaluated using NLR and platelet-to-lymphocyte ratio (PLR), calculated from peripheral blood counts obtained during the same baseline assessment.

Tumor characteristics were evaluated using multiphasic contrast-enhanced computed tomography and/or magnetic resonance imaging according to international recommendations. Recorded tumor variables included maximum tumor diameter, number of hepatic lesions, BCLC stage, and macrovascular

invasion. Macrovascular invasion was defined as radiological evidence of tumor invasion involving the major portal vein branches and/or hepatic veins.[14,15,18]

All clinical assessments, laboratory investigations, inflammatory marker measurements, MELD score calculations, radiological staging, and serum sampling for circRNA analysis were performed during the same baseline visit.

Clinical–inflammatory stratification

To integrate hepatic dysfunction and systemic inflammatory activity into a clinically applicable framework, patients were assigned to one of three exploratory clinical–inflammatory phenotypes based on the combined MELD score and NLR.

Phenotype I was defined as preserved hepatic function with low inflammatory activity and included patients. Phenotype III represented advanced clinical–inflammatory status. Patients who did not fulfill criteria for either Phenotype I or Phenotype III were classified as Phenotype II.

A hierarchical classification approach was applied to ensure mutually exclusive phenotype assignment. In cases of discordance between MELD score and NLR values, patients were assigned according to the higher-risk category.

Because MELD score and NLR constituted the proposed phenotype assignment criteria, differences in these variables across phenotypes were considered inherent characteristics of the classification algorithm rather than independent validation findings. Therefore, subsequent analyses focused on clinical characteristics not incorporated into phenotype assignment, including HCC distribution, tumor characteristics, BCLC stage, and macrovascular invasion.

Statistical analysis

All statistical analyses were performed using IBM SPSS Statistics version 26 (IBM Corp., Armonk, NY, USA). Statistical significance was defined as a two-sided P value < 0.05.

Data were initially examined for completeness, consistency, and distributional assumptions. Continuous variables were assessed for normality using the Shapiro–Wilk test together with visual inspection of histograms and Q–Q plots. Normally distributed variables are presented as mean ± standard deviation (SD), whereas nonnormally distributed variables are summarized as median and interquartile range (IQR). Categorical variables are presented as frequencies and percentages.

Comparisons between two independent groups were performed using the independent-samples t test for normally distributed continuous variables or the Mann–Whitney U test for nonnormally distributed variables. Comparisons among three independent groups were conducted using one-way analysis of variance with appropriate post hoc multiple-comparison testing for normally distributed variables or the Kruskal–Wallis test for nonparametric data. Associations between categorical variables were evaluated using the Pearson chi-square test or Fisher's exact test whenever the expected cell count was less than five.

Relationships between continuous variables were assessed using Spearman rank correlation coefficient. Correlation analyses were performed to evaluate associations among inflammatory indices, liver disease severity scores, tumor characteristics, and circulating *hsa_circ_101555* expression.

Multivariable binary logistic regression analysis was performed to identify factors independently associated with BCLC stage C among HCC patients. Variables considered clinically relevant or statistically significant in univariable analyses were included in the multivariable model after assessment for multicollinearity. Regression coefficients (β), standard errors, odds ratios, 95% confidence intervals (CIs), and corresponding P *values* were reported.

The discriminatory performance of individual biomarkers and multivariable models was evaluated using receiver operating characteristic (ROC) curve analysis. Areas under the ROC curve (AUCs) with corresponding 95% confidence intervals were calculated, and optimal cutoff values were determined using the Youden index. Pairwise comparisons between ROC curves were performed using the DeLong method.

Because MELD score and NLR constituted the variables used for the exploratory clinical–inflammatory phenotype assignment, ROC analyses were not performed to predict phenotype membership to avoid circularity. Instead, discriminant analyses evaluated the ability of MELD, NLR, and their combined continuous logistic regression to discriminate BCLC stage C disease among patients with HCC. The logistic regression model generated individual predicted probabilities of BCLC stage C disease. For classification purposes, predicted probabilities ≥0.50 were classified as positive for BCLC stage C disease, whereas predicted probabilities <0.50 were classified as negative.

The internal performance of the combined MELD–NLR model was evaluated using bootstrap resampling with 1,000 iterations to estimate optimism-corrected discrimination. Model calibration was assessed using the Hosmer–Lemeshow goodness-of-fit test. Overall classification performance was further summarized using sensitivity, specificity, and overall classification accuracy.

Bioinformatic selection and quantification of circulating hsa_circ_101555

The candidate circRNA *hsa_circ_101555* was selected before patient recruitment through a standardized bioinformatic workflow based on publicly available transcriptomic datasets. RNA sequencing datasets from HCC and normal liver tissues were retrieved from The Cancer Genome Atlas (TCGA), Gene Expression Omnibus (GEO), and the European Nucleotide Archive (ENA). Raw sequencing quality was assessed using FastQC, and sequence reads were aligned to the human reference genome using splice-aware alignment algorithms. Candidate circular RNAs were identified by detecting back-splice junctions using CircExplorer2. Differential expression analysis was performed using DESeq2 following normalization of sequencing counts. Candidate circRNAs were subsequently cross-referenced with circBase, circAtlas, circBank, and the published literature. Based on these analyses, *hsa_circ_101555* was selected as the candidate biomarker for clinical validation.

Primers were designed to specifically amplify the unique back-splice junction of *hsa_circ_101555* using Primer-BLAST (National Center for Biotechnology Information). Primer specificity was confirmed *in silico* against the human reference genome, and potential secondary structures were evaluated using the Integrated DNA Technologies (IDT) OligoAnalyzer tool. The primer sequences used were as follows:

Forward primer: 5′-AGTCTGACGTGACGTCGAGT-3′

Reverse primer: 5′-TCGACGTACTGAGCTCAGTA-3′

The expected polymerase chain reaction (PCR) amplicon size for *hsa_circ_101555* was 128 bp and was confirmed during assay optimization before analysis.

Peripheral venous blood (3 mL) was collected from each participant into serum separator tubes before the initiation of HCC-specific treatment. Samples were centrifuged at 4,000 rpm for 15 min, and serum aliquots were immediately stored at −80°C until molecular analysis.

Total RNA was extracted from serum samples using the miRNeasy Serum/Plasma Advanced Kit (Qiagen, Hilden, Germany; Cat. No. 217204) according to the manufacturer's instructions. Reverse transcription was performed using the miRCURY LNA RT Kit (Qiagen; Cat. No. 339340).

Circulating *hsa_circ_101555* expression was quantified by reverse transcription quantitative polymerase chain reaction (RT-qPCR) using RT² SYBR Green chemistry on a Rotor-Gene real-time PCR platform. The endogenous reference gene *ACTB* was selected following preliminary validation, which showed stable Ct values across all analyzed serum samples. Relative circRNA expression was calculated using the comparative 2^−ΔΔCt method and expressed as arbitrary units (AU).

Thermal cycling consisted of an initial activation step at 95°C for 10 min, followed by 40 amplification cycles of denaturation at 95°C for 15 s, annealing at 55°C for 30 s, and extension at 72°C for 30 s.

All PCR reactions were performed in duplicate, and no-template controls were included in every amplification run to exclude reagent contamination. Amplification specificity was confirmed by melting-curve analysis, which demonstrated a single sharp melting peak for each assay without evidence of nonspecific amplification or primer-dimer formation. Samples showing inconsistent duplicate amplification or inadequate amplification quality were repeated before inclusion in the final dataset.

Analytical reproducibility was evaluated using duplicate measurements performed on randomly selected serum samples. The assay demonstrated high intra-assay and inter-assay reproducibility, with low coefficients of variation and high intraclass correlation coefficients, supporting the reproducibility of the molecular measurements. The intra-assay coefficient of variation was 3.6%, while the inter-assay coefficient of variation was 5.2%. Agreement between repeated measurements was high, with an intraclass correlation coefficient of 0.96 (95% CI, 0.92–0.99).

Laboratory personnel responsible for RNA extraction and RT-qPCR analyses were blinded to all clinical, laboratory, radiological, and outcome data throughout molecular testing. Molecular analyses were completed before statistical analyses were initiated, and laboratory investigators were blinded until the study database was finalized, thereby minimizing the potential for measurement and observer bias. Radiological image interpretation, BCLC staging, and MELD score calculation were performed independently using routine clinical and imaging data before molecular analyses were completed and were therefore not influenced by circRNA results or phenotype assignment.

Sample size considerations

This study was designed as an exploratory (secondary analysis) cross-sectional investigation and represented the final phase of our translational research program. All eligible patients who presented consecutively during the study period were enrolled. No formal a priori sample size calculation was performed because the primary objective was exploratory biomarker evaluation and hypothesis generation.

The available sample allowed exploratory evaluation of associations between clinical–inflammatory phenotypes, circulating *hsa_circ_101555* expression, and advanced HCC features; however, the findings require external validation in larger independent cohorts.

Ethical considerations

The study was conducted under a research protocol approved by the Research Ethics Committee, Faculty of Medicine, Ain Shams University, Cairo, Egypt (approval no. FMASU MD 234/2022; approved in 2022). The study was conducted in accordance with the ethical principles of the Declaration of Helsinki (revised in 2024). Written informed consent was obtained from all participants before enrollment.

Results

Baseline characteristics of the study population

A total of 92 patients with chronic liver disease were included in the final analysis, comprising 30 patients with cirrhosis without HCC and 62 patients with radiologically confirmed HCC. Baseline demographic and laboratory characteristics are summarized in Table 1.

Table 1. Baseline characteristics of the study population

Variable	Cirrhosis (*n* = 30)	HCC (*n* = 62)	*P* value
Age (years), mean ± SD	56.4 ± 8.2	58.7 ± 7.9	0.184
Male sex, *n* (%)	12 (40.0%)	42 (67.7%)	0.011
Total bilirubin (mg/dL), mean ± SD	3.01 ± 2.63	1.28 ± 1.16	0.002
INR, mean ± SD	1.36 ± 0.18	1.14 ± 0.19	< 0.001
Serum albumin (g/dL), mean ± SD	3.07 ± 0.40	3.66 ± 0.54	< 0.001
AFP (ng/mL), median (IQR)	4.1 (2.8–6.2)	356 (85–1820)	< 0.001

AFP values are presented as median (interquartile range) because of their nonnormal distribution. Continuous variables were compared using the independent-samples *t* test or Mann–Whitney *U* test, as appropriate. AFP, alpha-fetoprotein; HCC, hepatocellular carcinoma; INR, international normalized ratio; IQR, interquartile range; SD, standard deviation

The mean age did not differ significantly between patients with cirrhosis and those with HCC (56.4 ± 8.2 vs. 58.7 ± 7.9 years, $P = 0.184$). However, the proportion of male patients was significantly higher in the HCC group than in the cirrhosis group (67.7% vs. 40.0%, $P = 0.011$).

Compared with patients with HCC, those with cirrhosis had

significantly greater impairment of hepatic synthetic function, reflected by higher serum bilirubin concentrations (3.01 ± 2.63 vs. 1.28 ± 1.16 mg/dL, $P = 0.002$), higher international normalized ratio values (1.36 ± 0.18 vs. 1.14 ± 0.19, $P < 0.001$), and lower serum albumin concentrations (3.07 ± 0.40 vs. 3.66 ± 0.54 g/dL, $P < 0.001$).

AFP concentrations were markedly higher among patients with HCC than among those with cirrhosis. Owing to the skewed distribution of AFP values, concentrations are presented as the median (interquartile range) and differed significantly between the two groups ($P < 0.001$).

Overall indices of liver disease severity are presented in Table 2. Across the entire study cohort, the mean MELD score was 11.39 ± 4.86. Half of the patients had moderate-to-severe underlying liver dysfunction, with 46 of 92 patients (50.0%) classified as Child–Pugh class B or C. 72 of 92 patients (78.2%) classified as ALBI grade 2 or 3, indicating that the cohort predominantly comprised patients with moderate-to-advanced chronic liver disease.

Table 2. Overall liver disease severity in the study population (*n* = 92)

Parameter	Value
MELD score, mean ± SD	11.39 ± 4.80
Child–Pugh class, *n* (%)	
• Class A	46 (50.0)
• Class B	35 (38.0)
• Class C	11 (12.0)
ALBI grade, *n* (%)	
• Grade 1	20 (21.7)
• Grade 2	44 (47.8)
• Grade 3	28 (30.4)

Values are presented as mean ± SD or number (%), as appropriate. ALBI, albumin–bilirubin; MELD, Model for End-Stage Liver Disease; SD, standard deviation

Inflammatory profile

Markers of systemic inflammation varied considerably across the study population. The mean NLR was 8.24 ± 4.73, the mean PLR was 142.6 ± 52.3, and the mean CRP concentration was 18.4 ± 9.7 mg/L (Table 3).

Correlation analyses demonstrated significant associations between inflammatory indices and markers of liver disease severity (Table 4). Higher NLR values were positively correlated with MELD score ($r = 0.62$, $P < 0.001$), serum bilirubin concentration ($r = 0.58$, $P < 0.001$), and tumor size among patients with HCC ($r = 0.61$, $P < 0.001$). In contrast, NLR showed a moderate inverse correlation with serum albumin concentration ($r = −0.51$, $P < 0.001$), consistent with an association between greater systemic inflammatory activity and poorer hepatic synthetic function.

Similarly, PLR demonstrated significant positive correlations

Table 3. Baseline inflammatory markers in the study population (*n* = 92)

Marker	Value
Neutrophil-to-lymphocyte ratio (NLR), mean ± SD	8.24 ± 4.67
Platelet-to-lymphocyte ratio (PLR), mean ± SD	142.6 ± 52.3
C-reactive protein (CRP), mg/L, mean ± SD	18.4 ± 9.7

Values are presented as mean ± standard deviation. CRP, C-reactive protein; NLR, neutrophil-to-lymphocyte ratio; PLR, platelet-to-lymphocyte ratio; SD, standard deviation

Table 4. Correlation between inflammatory markers and indices of disease severity

Variable	NLR (*r*)	PLR (*r*)	*P* value
MELD score	0.62	0.55	< 0.001
Total bilirubin	0.58	0.49	< 0.001
Serum albumin	−0.51	−0.46	< 0.001
Tumor size*	0.61	0.59	< 0.001

*Tumor size correlations were calculated among patients with HCC only (*n* = 62) using Spearman rank correlation coefficient. HCC, hepatocellular carcinoma; MELD, Model for End-Stage Liver Disease; NLR, neutrophil-to-lymphocyte ratio; PLR, platelet-to-lymphocyte ratio; r, Spearman rank correlation coefficient.

with MELD score ($r = 0.55$, $P < 0.001$), serum bilirubin ($r = 0.49$, $P < 0.001$), and tumor size ($r = 0.59$, $P < 0.001$), together with a negative correlation with serum albumin concentration ($r = −0.46$, $P < 0.001$). These findings indicate associations between systemic inflammatory activation and both hepatic dysfunction and tumor burden along the cirrhosis–HCC continuum.

Tumor characteristics among patients with HCC

Tumor characteristics of the 62 patients with HCC are summarized in Table 5. The mean maximum tumor diameter was 5.6 ± 2.3 cm. Multifocal disease was more common than solitary lesions, occurring in 38 patients (61.3%) compared with 24 patients (38.7%).

Macrovascular invasion was identified in 23 patients (37.1%), indicating a substantial proportion of patients with locally advanced disease. According to the BCLC staging system, 11 patients (17.7%) were classified as stage A, 23 (37.1%) as stage B, and 28 (45.2%) as stage C.

Overall, the HCC cohort was characterized by a predominance of intermediate-to-advanced stage disease, with frequent multifocal tumors and macrovascular invasion, consistent with the advanced clinical spectrum represented in this study.

Clinical–inflammatory phenotypic stratification

Patients were classified into three exploratory clinical–inflammatory phenotypes using a hierarchical algorithm based on baseline MELD score and NLR. Phenotype I included 25 patients (27.2%), Phenotype II included 33 patients (35.9%), and Phenotype III included 34 patients (37.0%) (Table 6).

As MELD score and NLR were incorporated into the proposed classification algorithm, differences in these variables across

Table 5. Tumor characteristics among patients with HCC (*n* = 62)

Variable	Value
Maximum tumor diameter (cm), mean ± SD	5.6 ± 2.3
Solitary lesion, *n* (%)	24 (38.7)
Multifocal disease, *n* (%)	38 (61.3)
Macrovascular invasion, *n* (%)	23 (37.1)
BCLC stage, *n* (%)	
• Stage A	11 (17.7)
• Stage B	23 (37.1)
• Stage C	28 (45.2)

Tumor staging was assigned according to the Barcelona Clinic Liver Cancer (BCLC) classification based on baseline radiological assessment before initiation of HCC-specific treatment. HCC, hepatocellular carcinoma; SD, standard deviation.

Table 6. Distribution of exploratory clinical–inflammatory phenotypes

Phenotype	Patients, *n* (%)
Phenotype I	25 (27.2)
Phenotype II	33 (35.9)
Phenotype III	34 (37.0)

Patients were classified using the hierarchical MELD–NLR algorithm described in the Materials and methods section. MELD, Model for End-Stage Liver Disease; NLR, neutrophil-to-lymphocyte ratio.

phenotype groups reflected expected characteristics of the classification system rather than independent validation findings. Therefore, subsequent analyses focused on clinical and tumor-related variables that were not included in phenotype assignment.

The distribution of underlying liver disease differed significantly across the three phenotypes (Table 7). The proportion of patients with HCC increased progressively from 40.0% in Phenotype I to 69.7% in Phenotype II and 85.3% in Phenotype III ($P < 0.001$), whereas cirrhosis without HCC predominated in the lower-risk phenotype.

Among patients with HCC, higher-risk phenotypes demonstrated a greater frequency of advanced tumor characteristics (Table 8). The proportion of patients with BCLC stage C disease increased from 10.0% in Phenotype I to 30.4% in Phenotype II and 69.0% in Phenotype III ($P < 0.001$). Likewise, macrovascular invasion became progressively more frequent across the phenotype spectrum, occurring in 10.0%, 30.4%, and 51.7% of patients with HCC in Phenotypes I, II, and III, respectively ($P = 0.012$).

Collectively, these findings indicate that the exploratory MELD–NLR clinical–inflammatory framework identified patient groups with progressively increasing frequencies of advanced HCC characteristics that were not used for phenotype assignment (Fig. 1).

Cross-sectional discrimination of BCLC stage C disease

Because MELD score and NLR were incorporated into the exploratory clinical–inflammatory phenotype classification, receiver operating characteristic (ROC) analyses were not performed to predict phenotype membership to avoid circularity. Instead, discriminant analyses evaluated the ability of MELD, NLR, and their combined continuous logistic regression to discriminate BCLC stage C disease among patients with HCC.

Among the 62 patients with HCC, 28 (45.2%) fulfilled BCLC stage C (Table 9, Fig. 2). ROC analyses demonstrated good discriminatory performance for both NLR and MELD score, with AUCs of 0.80 (95% CI, 0.69–0.90) and 0.77 (95% CI, 0.66–0.88), respectively (Table 10). PLR and CRP showed moderate discrimination, with AUCs of 0.71 (95% CI, 0.59–0.83) and 0.74 (95% CI, 0.62–0.85), respectively.

In the multivariable logistic regression model, both MELD score and NLR were independently associated with BCLC stage C disease (Table 11). The combined model achieved an apparent AUC of 0.90 (95% CI, 0.82–0.97), with a sensitivity of 85.7% and specificity of 82.4%. Internal validation using bootstrap resampling demonstrated minimal optimism (0.02), yielding an optimism-corrected AUC of 0.89. Calibration was satisfactory (Hosmer–Lemeshow $P = 0.61$), indicating acceptable calibration within this cohort.

Using a predicted probability threshold of 0.50, the combined MELD–NLR model correctly classified 52 of the 62 patients with HCC (83.9%), including 24 true-positive, 28 true-negative, 4 false-negative, and 6 false-positive classifications (Table 12).

Pairwise comparisons using the DeLong test showed a significantly higher AUC for the combined MELD–NLR model than for MELD score alone ($P = 0.021$), NLR alone ($P = 0.037$), PLR ($P < 0.001$), CRP ($P < 0.001$), and circulating *hsa_circ_101555* ($P < 0.001$) (Table 13).

Circulating hsa_circ_101555 expression and incremental discriminatory value

Circulating *hsa_circ_101555* expression was quantified in all study participants ($n = 92$), with a mean expression level of 6.96 ± 3.45 AU. Among patients with HCC, the mean expression level was 7.66 AU; expression levels varied according to tumor characteristics (Table 14). Patients with tumors ≤ 5 cm had significantly higher expression than those with tumors > 5 cm (9.29 ± 3.80 vs. 6.40 ± 3.35 AU, $P < 0.001$). Likewise, expression decreased progressively with advancing BCLC stage, with the highest levels observed in stage A disease and the lowest in stage C ($P < 0.001$).

Circulating *hsa_circ_101555* showed weak inverse correlations with systemic inflammatory markers, including NLR ($r = −0.331$, $P = 0.009$) and PLR ($r = −0.290$, $P = 0.022$), suggesting lower expression in patients with greater inflammatory activity. However, expression levels showed substantial overlap among the clinical–inflammatory phenotypes, and no significant differences were observed between phenotype groups (Fig. 3a).

When evaluated as an individual biomarker for discriminating BCLC stage C disease, *hsa_circ_101555* demonstrated modest discriminatory performance (AUC 0.69, 95% CI 0.57–0.81). Incorporation of *hsa_circ_101555* into the combined MELD–NLR model did not improve discriminatory performance, with the AUC remaining unchanged at 0.90 (Tables 15 and 16; Fig. 3b). The DeLong comparison showed that adding the biomarker did not significantly improve discrimination ($P = 0.79$).

Table 7. Distribution of liver disease categories according to clinical–inflammatory phenotype

Disease category	Phenotype I (*n* = 25)	Phenotype II (*n* = 33)	Phenotype III (*n* = 34)	*P value*
Cirrhosis without HCC, *n* (%)	15 (60.0)	10 (30.3)	5 (14.7)	< 0.001
HCC, *n* (%)	10 (40.0)	23 (69.7)	29 (85.3)	< 0.001

P values were calculated using the chi-square test for trend. HCC, hepatocellular carcinoma.

Table 8. Clinical and tumor characteristics according to clinical–inflammatory phenotypes

Variable	Phenotype I (*n* = 25)	Phenotype II (*n* = 33)	Phenotype III (*n* = 34)	*P* value
MELD score, mean ± SD†	8.50 ± 2.40	11.00 ± 3.10	13.89 ± 6.10	< 0.001
NLR, mean ± SD†	5.50 ± 2.60	8.00 ± 3.80	10.50 ± 5.50	< 0.001
BCLC stage C among HCC patients, n/N (%)	1/10 (10.0)	7/23 (30.4)	20/29 (69.0)	< 0.001
Macrovascular invasion among HCC patients, n/N (%)	1/10 (10.0)	7/23 (30.4)	15/29 (51.7)	0.012

†MELD score and NLR were incorporated into phenotype assignment and are presented to describe the classification algorithm rather than to validate it. Tumor-related variables were calculated among patients with HCC only. Cochran–Armitage trend test was used for *P* values in BCLC stage C and macrovascular invasion. BCLC, Barcelona Clinic Liver Cancer; HCC, hepatocellular carcinoma; MELD, Model for End-Stage Liver Disease; NLR, neutrophil-to-lymphocyte ratio; SD, standard deviation

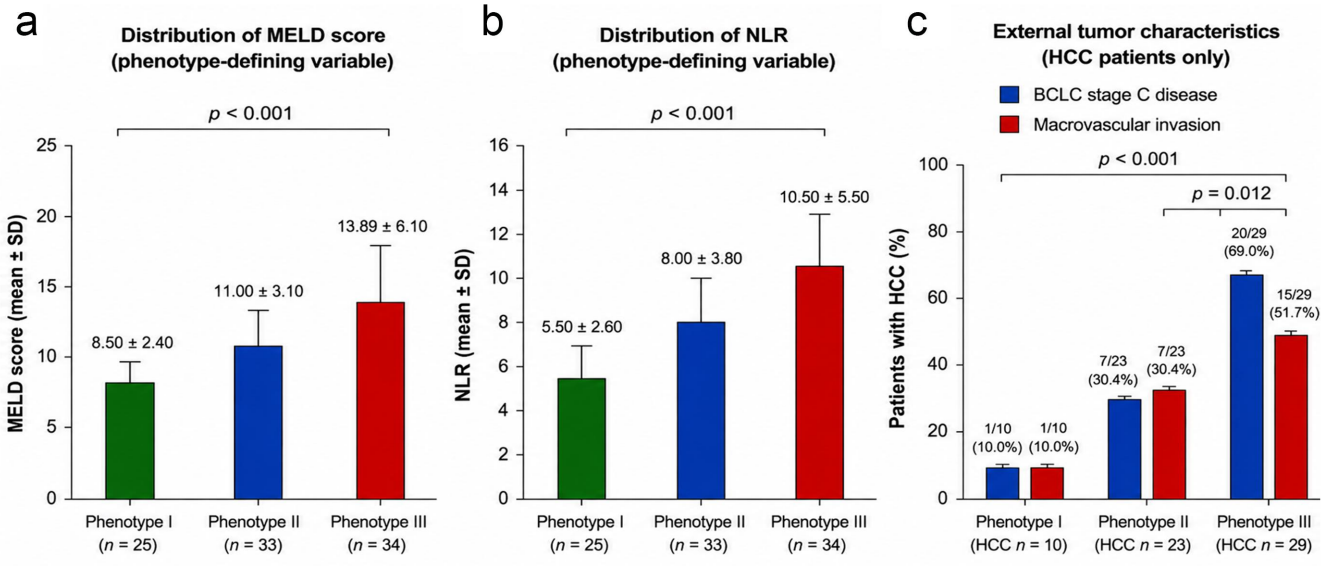

Fig. 1. Clinical characteristics according to MELD–NLR-based clinical–inflammatory phenotypes. Panels a and b show the mean (± SD) MELD scores and NLR values, respectively, across phenotype categories. Because these variables were incorporated into phenotype assignment, they represent classification characteristics rather than independent validation parameters. Panel c shows the proportions of patients with BCLC stage C disease and macrovascular invasion among patients with HCC. Comparisons used HCC-specific denominators. BCLC, Barcelona Clinic Liver Cancer; HCC, hepatocellular carcinoma; MELD, Model for End-Stage Liver Disease; NLR, neutrophil-to-lymphocyte ratio; SD, standard deviation.

Discussion

The present cross-sectional study evaluated an exploratory clinical–inflammatory classification integrating hepatic dysfunction and systemic inflammatory status along the cirrhosis–HCC continuum and examined its associations with clinicopathological characteristics and the potential incremental contribution of circulating *hsa_circ_101555*. Because MELD score and NLR were the variables used to construct the exploratory clinical–inflammatory phenotype framework, differences in these variables across phenotypes were expected by design and should not be interpreted as independent validation of the classification framework. Accordingly, the principal findings relate to clinical characteristics that were not incorporated into phenotype assignment. Patients in higher-risk clinical–inflammatory phenotypes had greater frequencies of advanced HCC features, including BCLC stage C disease and macrovascular

Table 9. Cross-tabulation of BCLC stage and macrovascular invasion among patients with HCC

BCLC stage	Macrovascular invasion (+)	Macrovascular invasion (−)	Total
Stage A/B	0	34	34
Stage C	23	5	28
Total	23	39	62

All 23 patients with macrovascular invasion were classified as BCLC stage C; therefore, macrovascular invasion did not identify additional patients beyond those with BCLC stage C disease. Accordingly, BCLC stage C disease (n = 28) was used as the outcome for the discrimination analyses. "+" indicates the presence of macrovascular invasion, whereas "−" indicates its absence. BCLC, Barcelona Clinic Liver Cancer; HCC, hepatocellular carcinoma.

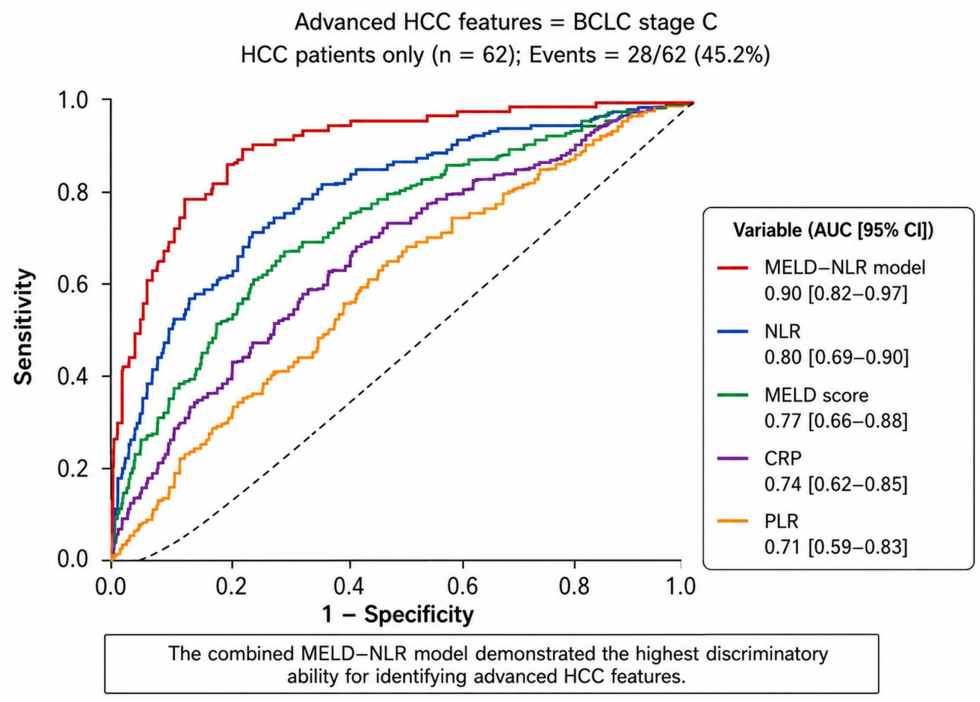

Fig. 2. Receiver operating characteristic curves for cross-sectional discrimination of BCLC stage C disease among patients with HCC (n = 62). ROC curves are shown for MELD score, neutrophil-to-lymphocyte ratio (NLR), platelet-to-lymphocyte ratio (PLR), C-reactive protein (CRP), and the combined MELD–NLR model. The combined MELD–NLR model had the largest area under the receiver operating characteristic curve (AUC, 0.90; 95% CI, 0.82–0.97). AUC, area under the receiver operating characteristic curve; BCLC, Barcelona Clinic Liver Cancer; CI, confidence interval; HCC, hepatocellular carcinoma; MELD, Model for End-Stage Liver Disease; ROC, receiver operating characteristic.

Table 10. ROC analysis for cross-sectional discrimination of BCLC stage C disease

Variable	AUC (95% CI)	Optimal cutoff	Sensitivity (%)	Specificity (%)	*P* value
NLR	0.80 (0.69–0.90)	> 4.3	78.6	76.5	< 0.001
MELD score	0.77 (0.66–0.88)	> 17	75.0	73.5	< 0.001
PLR	0.71 (0.59–0.83)	> 152	67.9	67.6	0.002
CRP	0.74 (0.62–0.85)	> 20 mg/L	71.4	70.6	< 0.001
Combined MELD–NLR model	**0.90 (0.82–0.97)**	—	**85.7**	**82.4**	< 0.001

Outcome: BCLC stage C disease. Population analyzed: patients with HCC only (n = 62). AUC, area under the receiver operating characteristic curve; BCLC, Barcelona Clinic Liver Cancer; CI, confidence interval; CRP, C-reactive protein; HCC, hepatocellular carcinoma; MELD, Model for End-Stage Liver Disease; NLR, neutrophil-to-lymphocyte ratio; PLR, platelet-to-lymphocyte ratio; ROC, receiver operating characteristic.

Table 11. Multivariable logistic regression model for discrimination of BCLC stage C

Variable	*β*	SE	Odds ratio (95% CI)	*P value*
Intercept	−6.82	1.88	—	< 0.001
MELD score	0.168	0.058	1.18 (1.05–1.33)	0.005
NLR	0.603	0.174	1.83 (1.30–2.58)	0.001

Model equation: logit(p) = −6.82 + 0.168 × MELD score + 0.603 × NLR; patients were classified as having BCLC stage C when the predicted probability was ≥ 0.50. *β*, regression coefficient; BCLC, Barcelona Clinic Liver Cancer; CI, confidence interval; HCC, hepatocellular carcinoma; MELD, Model for End-Stage Liver Disease; NLR, neutrophil-to-lymphocyte ratio; SE, standard error.

$$p = \frac{1}{1 + e^{-(-6.82+0.168MELD+0.603NLR)}}$$

Table 12. Classification performance of the combined MELD–NLR model

Observed outcome	Predicted BCLC stage C	Predicted BCLC stage A/B
Observed BCLC stage C (n = 28)	24	4
Observed BCLC stage A/B (n = 34)	6	28

Overall classification accuracy was 83.9% (52 of 62 patients). BCLC, Barcelona Clinic Liver Cancer; MELD, Model for End-Stage Liver Disease; NLR, neutrophil-to-lymphocyte ratio.

Table 13. Pairwise comparison of ROC curves using the DeLong test

Comparison	Difference in AUC	*P value*
MELD–NLR vs MELD	0.13	0.021
MELD–NLR vs NLR	0.10	0.037
MELD–NLR vs PLR	0.19	< 0.001
MELD–NLR vs CRP	0.16	< 0.001
MELD–NLR vs *hsa_circ_101555*	0.21	< 0.001

AUC, area under the receiver operating characteristic curve; CRP, C-reactive protein; MELD, Model for End-Stage Liver Disease; NLR, neutrophil-to-lymphocyte ratio; PLR, platelet-to-lymphocyte ratio; ROC, receiver operating characteristic

Table 14. Circulating *hsa_circ_101555* expression according to tumor characteristics

Variable	Category	*n*	Expression (AU), mean ± SD	*P value*
Tumor size	≤5 cm	27	9.29 ± 3.80	< 0.001
	> 5 cm	35	6.40 ± 3.35	
BCLC stage	A	11	10.63 ± 4.59	< 0.001
	B	23	7.42 ± 3.20	
	C	28	6.69 ± 3.05	
Correlation with NLR	Spearman r	—	−0.331	0.009
Correlation with PLR	Spearman r	—	−0.290	0.022

Population: patients with HCC (n = 62). Expression values are presented as arbitrary units (AU). Correlations were assessed using Spearman rank correlation coefficient. BCLC, Barcelona Clinic Liver Cancer; HCC, hepatocellular carcinoma; NLR, neutrophil-to-lymphocyte ratio; PLR, platelet-to-lymphocyte ratio; r, Spearman rank correlation coefficient; SD, standard deviation.

invasion, suggesting the potential clinical relevance of the proposed framework along the cirrhosis–HCC continuum.

Systemic inflammation is increasingly recognized as an important component of chronic liver disease and hepatocarcinogenesis. In the present study, higher NLR values were associated with more advanced clinicopathological

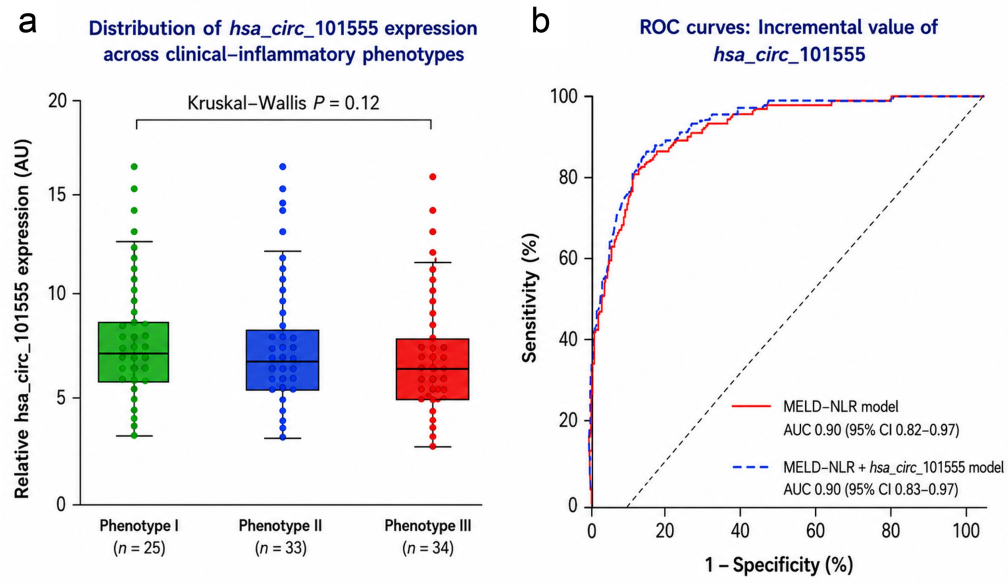

Fig. 3. Circulating hsa_circ_101555 expression and incremental discriminatory performance. (a) Distribution of circulating hsa_circ_101555 expression across the clinical–inflammatory phenotypes, showing substantial overlap and no significant differences between phenotype groups. Boxes indicate the median and interquartile range; whiskers extend to 1.5 times the interquartile range, and dots represent individual participants. (b) Receiver operating characteristic (ROC) curves comparing the combined MELD–NLR model with and without hsa_circ_101555 for discrimination of BCLC stage C disease. Adding hsa_circ_101555 did not improve discrimination (DeLong *P* = 0.79). AU, arbitrary units; AUC, area under the receiver operating characteristic curve; CI, confidence interval; HCC, hepatocellular carcinoma; IQR, interquartile range; MELD, Model for End-Stage Liver Disease; NLR, neutrophil-to-lymphocyte ratio.

Table 15. Discriminatory performance of *hsa_circ_101555* alone and in combination with clinical–inflammatory parameters

Model	AUC (95% CI)	Sensitivity (%)	Specificity (%)	*P value*
MELD	0.77 (0.66–0.88)	75.0	73.5	< 0.001
NLR	0.80 (0.69–0.90)	78.6	76.5	< 0.001
MELD–NLR	0.90 (0.82–0.97)	85.7	82.4	< 0.001
hsa_circ_101555	0.69 (0.57–0.81)	64.3	67.6	0.002
MELD–NLR + *hsa_circ_101555*	0.90 (0.83–0.97)	85.7	82.4	0.79†

Outcome: BCLC stage C. Population: patients with HCC only (n = 62). †Compared with the MELD–NLR model using the DeLong test. AUC, area under the receiver operating characteristic curve; BCLC, Barcelona Clinic Liver Cancer; CI, confidence interval; HCC, hepatocellular carcinoma; MELD, Model for End-Stage Liver Disease; NLR, neutrophil-to-lymphocyte ratio.

Table 16. Incremental value of *hsa_circ_101555* beyond the MELD–NLR model

Model comparison	ΔAUC	DeLong *P* value
MELD–NLR + *hsa_circ_101555* vs. MELD–NLR	0.002	0.79

ΔAUC, change in area under the receiver operating characteristic curve; MELD, Model for End-Stage Liver Disease; NLR, neutrophil-to-lymphocyte ratio.

characteristics, consistent with previous reports linking inflammatory activation with tumor aggressiveness and hepatic decompensation.[19-23] However, because of the cross-sectional design, these findings should be interpreted as associations rather than evidence of causality. Whether inflammatory activation contributes directly to disease progression or simply reflects more advanced disease cannot be determined from the present data and should be examined in prospective longitudinal studies.

An important objective of the present study was to determine whether circulating *hsa_circ_101555* provides incremental discriminatory information beyond routinely available clinical variables. Serum *hsa_circ_101555* expression was associated with smaller tumor size and earlier BCLC stage, suggesting that this biomarker may reflect aspects of tumor biology. However, substantial overlap in expression was observed across the clinical–inflammatory phenotypes, and the biomarker demonstrated only

modest cross-sectional discrimination of BCLC stage C disease. Furthermore, incorporation of *hsa_circ_101555* into the MELD–NLR model did not significantly improve discrimination in this cohort (ΔAUC = 0.002; DeLong $P = 0.79$). Collectively, these findings suggest that although *hsa_circ_101555* may provide biological insights into tumor behavior, it did not improve cross-sectional discrimination beyond routinely available laboratory parameters in the present cohort.[11]

The present findings should also be interpreted in the context of our previous investigations evaluating serum-derived *hsa_circ_101555* in HCC and chronic liver disease.[12,13] Those studies reported biological and diagnostic associations of *hsa_circ_101555* in different disease settings, whereas the current phase III study addressed a distinct clinical question by evaluating whether the biomarker contributes additional discriminatory information beyond an exploratory clinical–inflammatory framework along the cirrhosis–HCC continuum. Although the combined MELD–NLR model demonstrated higher discrimination than *hsa_circ_101555* alone, the findings should be regarded as exploratory and require confirmation and external validation in larger multicenter cohorts.

From a clinical perspective, these findings suggest that routinely available indices of hepatic reserve and systemic inflammatory activity may be useful for cross-sectional assessment of disease severity along the cirrhosis–HCC continuum. Because MELD score and NLR are widely available and inexpensive laboratory parameters, the proposed framework may represent a practical approach for clinical characterization in settings where molecular testing is not readily accessible. Nevertheless, this classification was internally derived and should be considered exploratory until externally validated. Future multicenter studies incorporating larger patient populations, additional circulating biomarkers, and prospective follow-up are required to determine whether molecular markers provide clinically meaningful incremental value beyond established clinical models.

Limitations

This study has several limitations. First, the cross-sectional design precludes assessment of temporal relationships, disease progression, or prognostic performance. Because prospective screening logs were not maintained, the total number of screened but non-enrolled patients could not be accurately reconstructed. Second, the relatively small sample size from a single tertiary referral center may limit generalizability and increase the risk of model overfitting despite internal bootstrap validation. Third, only one circulating circRNA was evaluated; therefore, these findings should not be generalized to other molecular biomarkers. Formal hemolysis assessment was not performed; therefore, a potential influence of occult sample hemolysis on circulating RNA measurements cannot be completely excluded despite standardized sample processing procedures. Fourth, the proposed clinical–inflammatory phenotypes were exploratory and hypothesis-generating but internally evaluated and require external validation before clinical implementation. Fifth, although bootstrap resampling demonstrated stable internal model performance, no independent external validation cohort was available. Finally, the study population excluded patients with active infection, inflammatory disorders, and hematological diseases because these conditions substantially influence inflammatory biomarkers; therefore, the applicability of the proposed framework may be limited to comparable clinical settings.

Conclusions

In this exploratory single-center cross-sectional study, the MELD–NLR-based clinical–inflammatory framework identifies patient groups with differing frequencies of advanced HCC features and provides a simple approach for clinical risk stratification. Circulating *hsa_circ_101555* provides no incremental discriminatory value beyond routinely available clinical–inflammatory parameters, and both the framework and biomarker findings require external validation before clinical application.

Supporting information

Supplementary material for this article is available at https://doi.org/10.14218/GE.2026.00023.

Acknowledgments

The authors express sincere gratitude to the staff of the Tropical Medicine Department, Ain Shams University Hospital, Egypt, for the technical and administrative support.

Funding

This research received no specific grant from any funding agency in the public, commercial, or not-for-profit sectors.

Conflict of interest

The authors declare no competing interests.

Author contributions

Conceptualization, study design, data analysis, and drafting the manuscript (NB); data collection and interpretation (MSG); laboratory and molecular data processing and validation (NEK); supervision and validation (ATAM, HEDMS). All authors reviewed and approved the final manuscript.

Ethical statement

The study was conducted under a research protocol approved by the Research Ethics Committee, Faculty of Medicine, Ain Shams University, Cairo, Egypt (approval no. FMASU MD 234/2022; approved in 2022). It was conducted in accordance with the ethical principles of the Declaration of Helsinki (revised in 2024). Written informed consent was obtained from all participants before enrollment.

Data sharing statement

The datasets generated and/or analyzed during the current study are not publicly available due to ethical and institutional restrictions. Data access requests may be considered on a case-by-case basis, subject to institutional policies, ethical approval, and

patient confidentiality requirements.

References

[1] Villanueva A. Hepatocellular Carcinoma. N Engl J Med 2019;380(15): 1450–1462. DOI: 10.1056/NEJMra1713263, PMID: 30970190.

[2] Sung H, Ferlay J, Siegel RL, Laversanne M, Soerjomataram I, Jemal A, *et al*. Global Cancer Statistics 2020: GLOBOCAN Estimates of Incidence and Mortality Worldwide for 36 Cancers in 185 Countries. CA Cancer J Clin 2021;71(3):209–249. DOI: 10.3322/caac.21660, PMID: 33538338.

[3] Llovet JM, Kelley RK, Villanueva A, Singal AG, Pikarsky E, Roayaie S, *et al*. Hepatocellular carcinoma. Nat Rev Dis Primers 2021;7(1):6. DOI: 10.1038/s41572-020-00240-3, PMID: 33479224.

[4] Kamath PS, Kim WR; Advanced Liver Disease Study Group. The model for end-stage liver disease (MELD). Hepatology 2007;45(3): 797–805. DOI: 10.1002/hep.21563, PMID: 17326206.

[5] Pugh RN, Murray-Lyon IM, Dawson JL, Pietroni MC, Williams R. Transection of the oesophagus for bleeding oesophageal varices. Br J Surg 1973;60(8):646–649. DOI: 10.1002/bjs.1800600817, PMID: 4541913.

[6] Reig M, Forner A, Rimola J, Ferrer-Fàbrega J, Burrel M, Garcia-Criado Á, *et al*. BCLC strategy for prognosis prediction and treatment recommendation: The 2022 update. J Hepatol 2022;76(3):681–693. DOI: 10.1016/j.jhep.2021.11.018, PMID: 34801630.

[7] Forner A, Reig M, Bruix J. Hepatocellular carcinoma. Lancet 2018; 391(10127):1301–1314. DOI: 10.1016/S0140-6736(18)30010-2, PMID: 29307467.

[8] Balkwill FR, Mantovani A. Cancer-related inflammation: common themes and therapeutic opportunities. Semin Cancer Biol 2012; 22(1):33–40. DOI: 10.1016/j.semcancer.2011.12.005, PMID: 22210179.

[9] Crusz SM, Balkwill FR. Inflammation and cancer: advances and new agents. Nat Rev Clin Oncol 2015;12(10):584–596. DOI: 10.1038/nrclinonc.2015.105, PMID: 26122183.

[10] Hung HC, Lee JC, Cheng CH, Wu TH, Wang YC, Lee CF, *et al*. Impact of neutrophil to lymphocyte ratio on survival for hepatocellular carcinoma after curative resection. J Hepatobiliary Pancreat Sci 2017;24(10):559–569. DOI: 10.1002/jhbp.498, PMID: 28846835.

[11] Gu X, Zhang J, Ran Y, Pan H, Jia J, Zhao Y, *et al*. Circular RNA hsa_circ_101555 promotes hepatocellular carcinoma cell proliferation and migration by sponging miR-145-5p and regulating CDCA3 expression. Cell Death Dis 2021;12(4):356. DOI: 10.1038/s41419-021-03626-7, PMID: 33824281.

[12] Gado MS, Moez ATA, El-Khazragy N, Salem HEDM, Badwei N. The potential oncogenic role of serum-derived hsa_circ_101555 as a non-invasive diagnostic/prognostic marker in patients with hepatocellular carcinoma. Gene Expr 2025;24(2):102–118. DOI: 10.14218/GE.2025.00012.

[13] Badwei N, Moez ATA, El-Khazragy N, Gado MS. Serum-derived hsa_circ_101555 as a diagnostic biomarker in non-hepatocellular carcinoma chronic liver disease: A phase II cross-sectional study. Gene Expr 2025;24(4):e00040. DOI: 10.14218/GE.2025.00040.

[14] European Association for the Study of the Liver. EASL Clinical Practice Guidelines on the management of hepatocellular carcinoma. J Hepatol 2025;82(2):315–374. DOI: 10.1016/j.jhep.2024.08.028, PMID: 39690085.

[15] Singal AG, Llovet JM, Yarchoan M, Mehta N, Heimbach JK, Dawson LA, *et al*. AASLD Practice Guidance on prevention, diagnosis, and treatment of hepatocellular carcinoma. Hepatology 2023;78(6): 1922–1965. DOI: 10.1097/HEP.0000000000000466, PMID: 37199193.

[16] Johnson PJ, Berhane S, Kagebayashi C, Satomura S, Teng M, Reeves HL, *et al*. Assessment of liver function in patients with hepatocellular carcinoma: a new evidence-based approach-the ALBI grade. J Clin Oncol 2015;33(6):550–558. DOI: 10.1200/JCO.2014.57.9151, PMID: 25512453.

[17] Hiraoka A, Kumada T, Kudo M, Hirooka M, Tsuji K, Itobayashi E, *et al*. Albumin-Bilirubin (ALBI) Grade as Part of the Evidence-Based Clinical Practice Guideline for HCC of the Japan Society of Hepatology: A Comparison with the Liver Damage and Child-Pugh Classifications. Liver Cancer 2017;6(3):204–215. DOI: 10.1159/000452846, PMID: 28626732.

[18] Kinoshita A, Onoda H, Fushiya N, Koike K, Nishino H, Tajiri H. Staging systems for hepatocellular carcinoma: Current status and future perspectives. World J Hepatol 2015;7(3):406–424. DOI: 10.4254/wjh.v7.i3.406, PMID: 25848467.

[19] Bernardi M, Moreau R, Angeli P, Schnabl B, Arroyo V. Mechanisms of decompensation and organ failure in cirrhosis: From peripheral arterial vasodilation to systemic inflammation hypothesis. J Hepatol 2015;63(5):1272–1284. DOI: 10.1016/j.jhep.2015.07.004, PMID: 26192220.

[20] Arroyo V, Moreau R, Kamath PS, Jalan R, Ginès P, Nevens F, *et al*. Acute-on-chronic liver failure in cirrhosis. Nat Rev Dis Primers 2016; 2:16041. DOI: 10.1038/nrdp.2016.41, PMID: 27277335.

[21] Pinato DJ, Stebbing J, Ishizuka M, Khan SA, Wasan HS, North BV, *et al*. A novel and validated prognostic index in hepatocellular carcinoma: the inflammation based index (IBI). J Hepatol 2012; 57(5):1013–1020. DOI: 10.1016/j.jhep.2012.06.022, PMID: 22732513.

[22] Tang J, Yan Z, Feng Q, Yu L, Wang H. The Roles of Neutrophils in the Pathogenesis of Liver Diseases. Front Immunol 2021;12:625472. DOI: 10.3389/fimmu.2021.625472, PMID: 33763069.

[23] Maccali C, Augustinho FC, Zocche TL, Silva TE, Narciso-Schiavon JL, Schiavon LL. Neutrophil-Lymphocyte Ratio Predicts Short-Term Mortality in Patients Hospitalized for Acute Decompensation of Cirrhosis. Arq Gastroenterol 2021;58(2):131–138. DOI: 10.1590/S0004-2803.202100000-23, PMID: 34287528.